Design of BIPTEM: an airborne B field IP and TEM system

James Macnae*
CD3D
Melbourne
jcm@c3dmap.com

Terry Kratzer
CD3D / Biptem
Melbourne
terry@biptem.com

Duncan Massie
Monex Geoscope
duncan.massie@
monexgeoscope.com.au

Paul Rogerson
Thomson Airborne
Griffith, NSW
paul@thomsonair.com

SUMMARY

The BIPTEM project was funded by several companies and developed a 1 MAm^2 transmitter which was tested with a concentric loop B field inductive magnetometer in 2017. A report on the system was presented at AEM18. With the rotation sensing and inertial navigation technology available at that time, motion noise corrections to the collected data did not perform well enough to justify further substantial investment and the project was mothballed. Following improvements in fibre-optic technology, and the announced future commercial availability of breakthrough quantum rotation sensors, Newmont funded research to improve the BIPTEM system and test its ability to map IP targets.

Many experiments and flight tests were conducted, and extensive software developments were undertaken to bring the system to full operation. Parallel modelling and ground experiments showed that the optimum system for IP effect detection has a large Tx and a horizontal component Rx (separated by about 300m in the Slingram geometry.

Key words: B field TEM Airborne IP Slingram

INTRODUCTION

Initial developments towards an airborne IP system were conducted from 2011-2016 in AMIRA Projects P1036 and P1036a. The AMIRA project developed and tested airborne electric field sensors and the 3-component RMIT University ARMIT B field sensor, but the RMIT proposal to continue development in P1036b was not funded. Independently, Source Geophysics, Monex Geoscope and Thomson Aviation developed the hardware for an AEM/AIP transmitter and receiver to house the ARMIT B field sensors.

Post the AMIRA projects, tests using a different (BIPTEM) inductive magnetometer with concentric loop geometry followed in 2017, but the available Russian molecular electronic technology (MET) rotation sensors proved inadequate to measure rotations accurately enough for the required corrections to motion-noise affected B field data. The project was then mothballed, with a watching brief focussed on rotation measurement technology.

In 2021, new inertial navigation sensors (INS) came on the market, and inexpensive sensors were announced for future (2023) commercialisation at an order of magnitude or more increased sensitivity; with a fraction of the cost, size and weight of other technologies With technology becoming available to address the shortcomings of the 2017 BIPTEM experiments, Newmont Inc, CD3D, Thomson Airborne and Monex Geoscope agreed to fund further development and field testing of the BIPTEM system.

SYSTEM DESIGN

Choice of Sensor

There are several choices to be made in an airborne EM system that is designed to measure IP effects. There are potentially 3 possible sensor choices to measure EM fields containing IP information. These and the relevant considerations are
Electric E field sensors (1). Theoretically the electric field is much more sensitive to IP effects than the magnetic field which requires significant current flow to be detectable. One implementation of such sensors were investigated over a decade ago in AMIRA Project P1036, and while the sensors had sufficient sensitivity, atmospheric signals (coupling to rapidly varying earth-ionosphere electric field, wind carried charge on dust particles) dominated observed responses
Coil dB/dt sensors (2) almost universally used in airborne EM systems. These sensors have a response that falls off as 1/f towards low frequencies, and hence have reduced sensitivity to the slow decays characteristic of IP effects.
Magnetometers (3) measuring B fields which are much more sensitive to IP effects that dB/dt sensor (Figure 1)

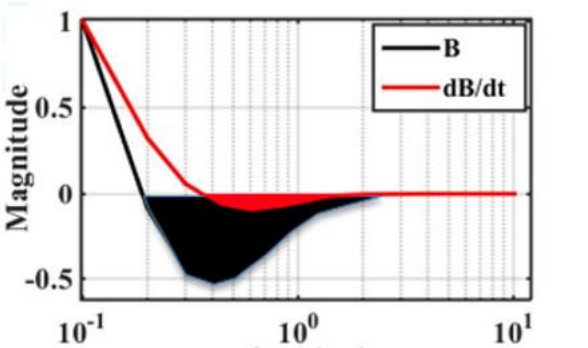

Figure 1: Comparison over polarizable ground of measured decays between coil and SQUID sensors using the same transmitter and receiver locations.

There are 3 B field vector sensor types commercially used in electromagnetic geophysics: Fluxgates (which are too noisy), SQUIDS (logistically inconvenient, Foley et al, 1999, Stolz et al, 2022) and Inductive Magnetometers. (commonly used in MT and AMT systems). There are also two types of inductive magnetometers: feedback (e.g. Zonge) or current sensing (e.g. ARMIT, Macnae and Kratzer, 2013). Inductive magnetometers have internal noise level substantially less than ambient (sferic) and rotation noise, so were chosen for BIPTEM.

Motion Noise

Having settled on an inductive B field sensor, we chose a cube geometry based on an expired/abandoned UNB patent (duPuis et al, 2008) which ensured orthogonality between inductive magnetometers (Figure 2). Figure 3 shows a suspended test jig of the sensor layout on a plywood cube with attached GPS and inertial navigation IMU sensors.

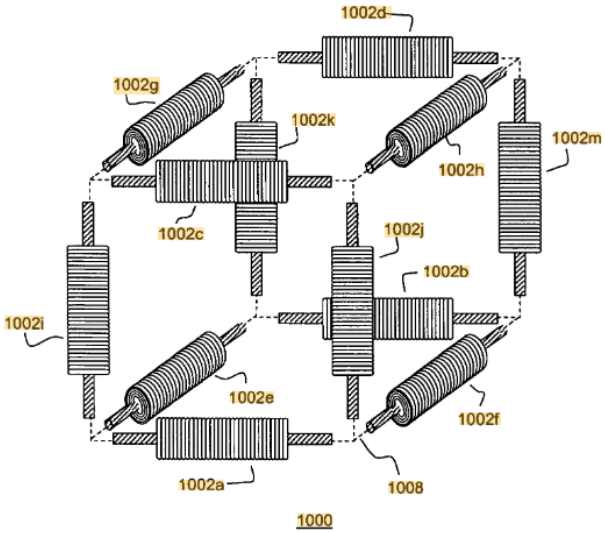

Figure 2: Patent US7375529B2 Figure 10 depicting a good layout for inductive magnetometer sensors with a high moment of inertia (resistance to rotation)

The reason motion (strictly rotation) noise is important is that magnetometers couple to the earth's magnetic field B_E, nominally say 50,000 nT in amplitude. BIPTEM inductive magnetometers have a sensitivity better than 0.5 pT, which is more than 100 million times smaller than B_E. Figure 4 illustrates that only rotations about the x and y axes affect the magnitude of the z component measurement Bz due to the earth's field.

It is of note that inductive magnetometers do not have "DC" magnetic field sensitivity, and as such do not detect B_E directly, but rather measure any changes due to coupling in the bandwidth of the sensor/system from say 0.1 Hz to 50 kHz.

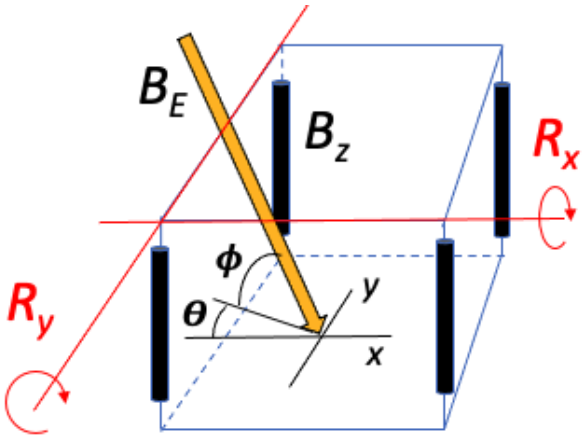

Figure 4: B_z sensor coupling to the Earth's magnetic field B_E changes with rotations R about the x and y axes, and can be expressed as trigonometrical functions of the rotations R_x, R_y and coupling angles θ, ϕ .

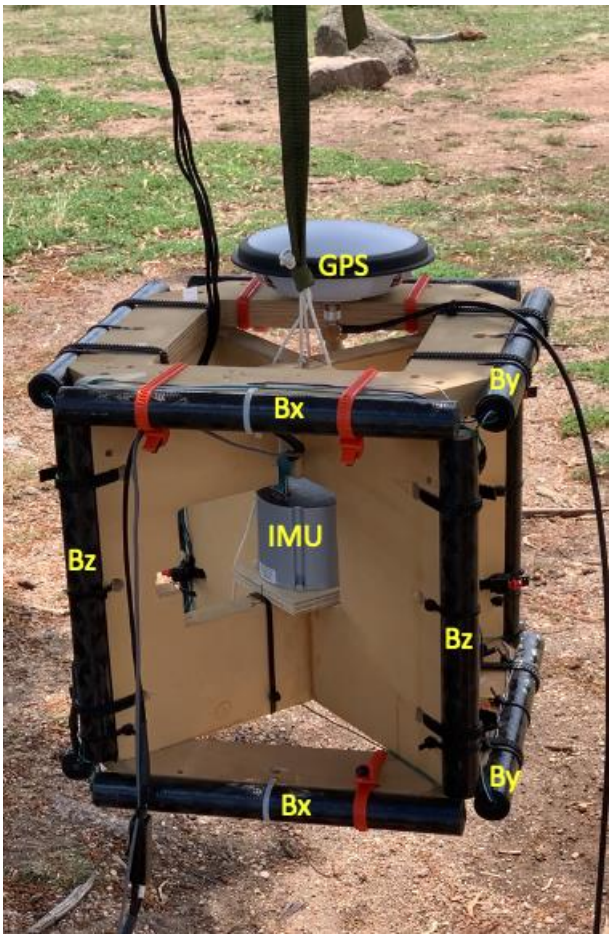

Figure 3: Test jig with 3 (x,y,z) component B field sensors with rotation measuring hardware.

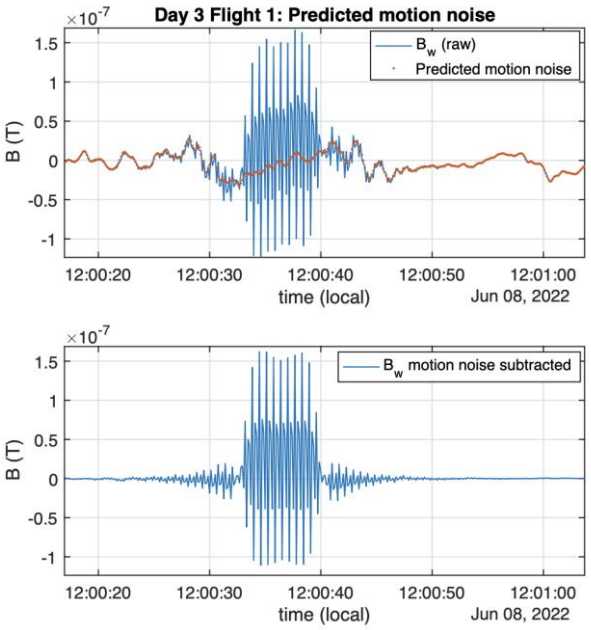

Figure 5: Effect of rotation corrections (motion noise) on measured B field during overflight of a transmitter

Figure 5 shows the result of motion noise corrections using about 50 seconds of streamed data with measured rotations and an assumed background magnetic field. Quite clear is that away from the transmitter, the predicted response matches the observed data, and that corrections reduce the variations seen in the measured data

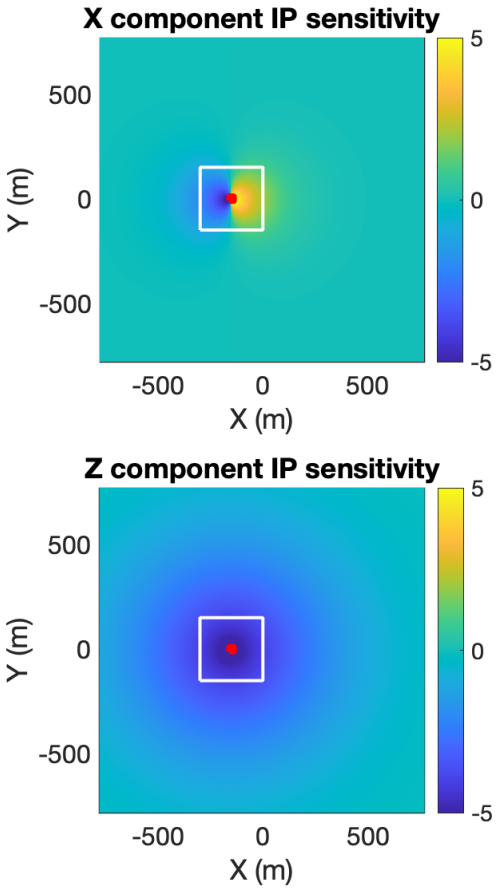

Figure 6: A central x directed horizontal sensor has equal and opposite sensitivity to the circulating EM induced current and reverse polarization currents either side of it. If the surficial polarizable conductor is uniform, then there is no net response in the X (or Y) components at the central position. A vertical Z component sensor responds to circulating reversed IP currents from a large region within and just outside the transmitter loop.

System Geometry Considerations

Most published studies of IP effects as seen from inductive EM sources have used coil sensors measuring the rate of change of the magnetic field dB/dt. Most IP effects seen in ground EM have been attributed to clays. Smith and West (1988) outline the three requirements for IP effects to significantly exceed the responses from EM induction. They can be simplified in time domain to:

1) The transmitter must couple well to a regional or local conductor so that induced polarizing currents are large at early delay times
2) The induced EM current must decay close to zero within the measured time window
3) The polarization current must be well coupled to the receiver

The most common case where these 3 conditions are met has been the Z component of coincident or concentric loop geometry used on the ground or in helicopter TEM surveys (Macnae, 2016) with sensitivity illustrated in Figure 6.

In the case of Slingram geometry (moving Tx with separated Rx) we will see that a large loop transmitter and a horizontal X component receiver satisfy these 3 conditions. This geometry was also recommended in the duPuis et al (2004) patent application as illustrated in Figure 7.

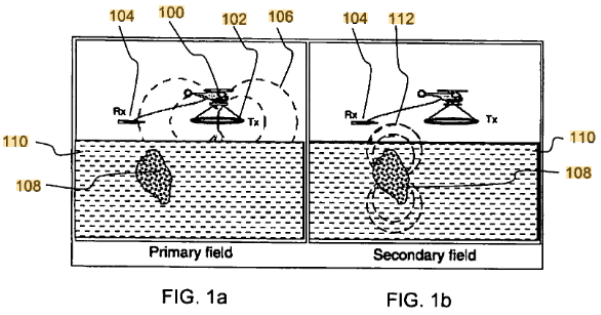

Figure 7. Suggested survey geometry from Patent US7375529B2 to minimise primary and maximise secondary field.

Figure 8 shows the sensitivity to IP effects of a magnetic field sensor located 300 m from a transmitter loop. This calculation shows that the x component has simple coupling to any IP reversed currents in the near surface.

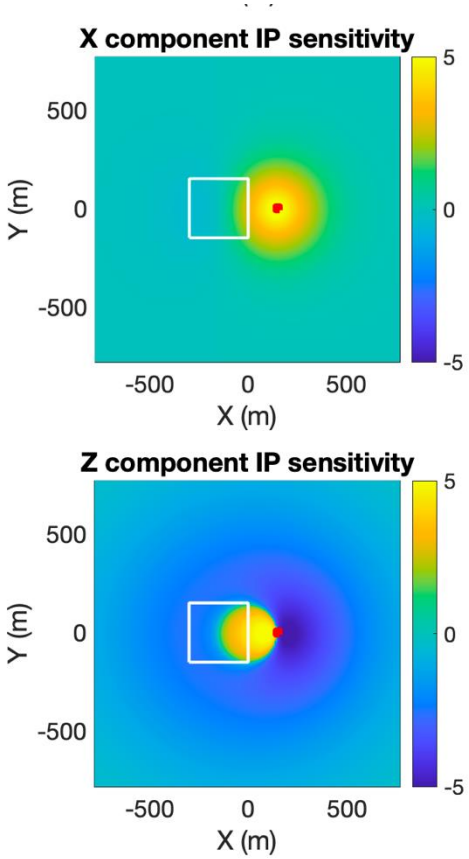

Figure 8: Slingram geometry X and Z component sensitivity to a 40 m deep polarizable sheet conductor. This incidentally would be the sensitivity of an airborne Slingram system flying at a height of 40 m over a surficial polarizable conductor. The x component is simply coupled to the smoke ring current, whereas the Z component has both positive and negative contributions.

Figure 9 presents a Bz vertical component profile flown over a transmitter loop operating with a 50% duty-cycle and 12.5 Hz repetition rate. The typical pattern of crossovers migrating away from the transmitter on either side is inductive of the conductive regolith in this location. The negatives located directly under the transmitter at late delay times (yellow profiles) indicate the presence on polarizable near-surface material.

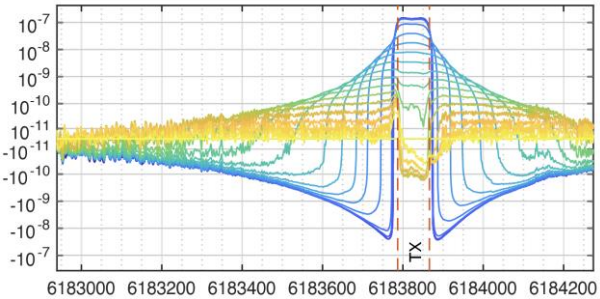

Figure 9. 12.5 Hz Z component data from a profile flown directly over a ground Tx has late time negative indicative of polarizable clays in the regolith with τ_{IP} = 15 ms

Figures 10 and 11 show vertical Bx and horizontal Bh component decays measured in a ground survey with a B field sensor and Slingram geometry. Consistent with sensitivity analysis that Bz IP anomalies may have either sign or be zero. The Bz component has a far smaller time window where negative IP effects dominate the EM decay.

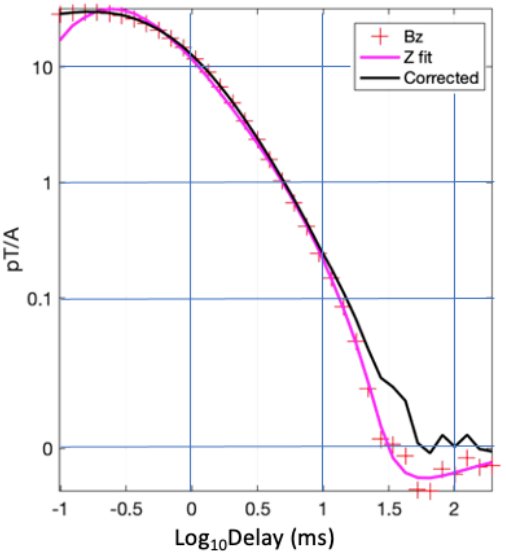

Figure 10: Bz decay 300 m from Tx loop. There is a small IP response visible at late delays. The black profile shows a corrected EM decay. Both measured and corrected data appear noisy at late delays on the logarithmic vertical scale.

FIELD TEST

A field test of the BIPTEM system in Slingram mode is to be conducted on April 19th, just after the deadline for abstract submission. Field testing requires an airborne transmitter as well as separated receiver, and we have designed and tested a 1

MAm^2 rigid transmitter to provide sufficient dipole Moment for effective data collection (Figure 12). Because the induced current "smoke ring" moves downwards and outwards, and it is necessary to have a receiver well-coupled to the reversed IP currents, we will use two helicopters to carry the transmitter and receiver (Figure 13)

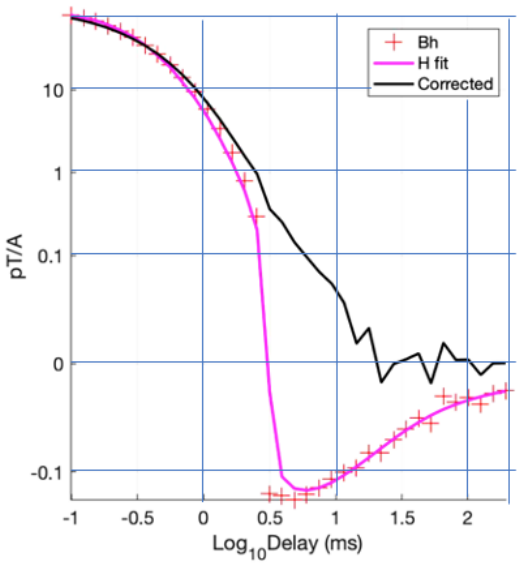

Figure 11: Corresponding Bx decay 300 m from Tx loop. There is a much larger IP response visible from medium to late delays. Again, noise is evident at late delays in the original and corrected data.

Figure 12: The transmitter in flight, with a 3 component BIPTEM sensor in the centre

CONCLUSIONS

Measuring airborne B fields to detect IP effects (and excellent conductors) presented a large number of challenges. These included design of a transmitter loop and sensor suspension systems that do not conflict with patents in the field. The biggest challenge however is measurement of rotations and the Earth's field to sufficient accuracy to permit rotation noise corrections.

Many experiments and flight tests have been conducted with prototype, and extensive software developments were undertaken to bring the system to full operation. Parallel modelling and ground experiments showed that the optimum system for IP effect detection has a large Tx and a horizontal component Rx (separated by about 300 m in the Slingram geometry.

ACKNOWLEDGMENTS

We thank Greg Walker for his confidence in our proposed technology and Newmont for funding this research.

REFERENCES

Du, S., Y. Zhang, Y. Pei, K. Jiang, L. Rong, C. Yin, Y. Ji , and X. Xie. (2018), Study of transient electromagnetic method measurements using a superconducting quantum interference device as B sensor receiver in polarizable survey area, GEOPHYSIC 83, https://doi.org/10.1190/geo2017-0197.1

Foley, C., K. Leslie, R. Binks, C. Lewis, W. Murray, G. Sloggett, S. Lam, B. Sankrithyan, N. Savvides, A. Katzaros, K. Muller, E. Mitchell, J. Pollock, J. Lee, D. Dart, R. Barrow, M. Asten, A. Maddever, G. Panjkovic, M. Downey, C. Hoffman, R. Turner. "Field trials using HTS SQUID magnetometers for ground-based and airborne geophysical applications," in IEEE Transactions on Applied Superconductivity, vol. 9, no. 2, pp. 3786-3792, June 1999, doi: 10.1109/77.783852.

Macnae J., and T. Kratzer, 2013, Joint sensing of B and dB/dt responses, ASEG2013 - 23rd Geophysical Conference

Macnae, J., 2016, Quantifying airborne Induced Polarization effects in helicopter time domain electromagnetics, Journal of Applied Geophysics 135, 495-502

R.S. Smith and G.F. West (1988) An explanation of abnormal TEM responses: coincident-loop negatives, and the loop effect. Exploration Geophysics 19(3) 435 - 446

Stolz, R, M Schifer, M. Becken, A. Thiede, M. Schneider G. Chubak P. Marsden A. Braña Bergshjorth M. Schaefer, O. Terblanche, 2022, SQUIDs for magnetic and electromagnetic methods in mineral exploration; Mineral Economics https://doi.org/10.1007/s13563-022-00333-3

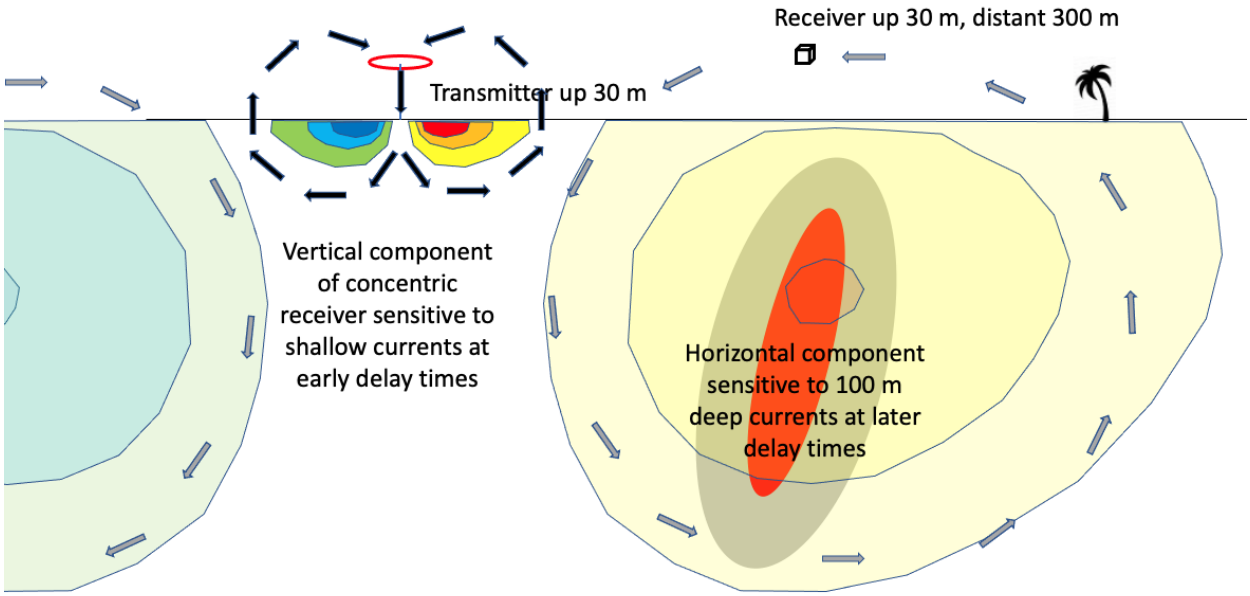

Figure 13. Currents induced in a background half-space below the transmitter location are shallow. The induced currents spread down and out, and having a receiver 300m behing the transmitter is optimum to detect induced currents (and thus reversed IP currents due to e.g. sulphides) at depths of 100 m or more